

Josephson effect test for triplet pairing symmetry

N. Stefanakis

Department of Physics, University of Crete, P.O. Box 2208, GR-71003, Heraklion, Crete, Greece

(November 11, 2018)

Abstract

The critical current modulation and the spontaneous flux of the vortex states in corner Josephson junctions between Sr_2RuO_4 and a conventional s -wave superconductor are calculated as a function of the crystal orientation, and the magnetic field. For Sr_2RuO_4 we assume two nodeless p -wave pairing states. Also we use the nodal f -wave states $B_{1g} \times E_u$ and $B_{2g} \times E_u$, and one special p -wave state having line nodes. It is seen that the critical current depends solely on the topology of the gap.

I. INTRODUCTION

During recent years, a renewed interest has been realized for unconventional superconductivity in Sr_2RuO_4 (SRO) [1]. This material has a layered structure and is a two dimensional Fermi liquid, with similarities to ^3He , that shows p -wave superfluidity. Knight-shift measurements suggest that unconventional superconductivity with pairing in the triplet channel is realized [2]. The time-reversal symmetry is violated for this state. This is consistent with the discovery of internal magnetic fields in the superconducting phase by μSR measurement [3]. Also specific-heat measurements support the scenario of line nodes within the superconducting gap as in the high- T_c cuprate superconductors [4]. Moreover thermal-conductivity measurements indicate the presence of horizontal lines of nodes [5]. The argument for unconventional superconductivity in SRO is further supported by the variation of T_c with nonmagnetic impurities [6].

The tunneling effect in ferromagnet-triplet-superconductor junctions can be used to determine the nodal structure of the pair potential and to distinguish the proposed pairing states. When the interface is normal to the ab plane, for two-dimensional order parameters, tunneling peaks are formed due to bound states that depend both on the surface orientation and the quasiparticle trajectory angle [7]. For three dimensional order parameters the tunneling spectra is sensitive to the orientation of the interface [8].

The Josephson effect has been observed experimentally in bilayer junctions $\text{Pb}/\text{Sr}_2\text{RuO}_4/\text{Pb}$, where a sharp drop of the critical current I_c is observed below the transition temperature of Sr_2RuO_4 [9]. This anomalous effect originates from the competition between the positive Josephson coupling strength between the two singlet superconductors and the negative one due to the singlet-/triplet-superconductor coupling [10]. Also in Ref. [11] it is argued that the Josephson coupling between a conventional s -wave superconductor In and Sr_2RuO_4 is allowed in the in-plane direction, but not in the c axis. The conclusion is that the pairing state in that case has to be a nodeless p -wave state.

In order to distinguish the pairing states with a two-dimensional order parameter, in

the present paper we study the static properties of a two-dimensional corner junction between SRO and a conventional s -wave superconductor. This is done by mapping the two dimensional (2D) junction into two single junctions, connected in parallel, by introducing an extra relative phase in one part of this junction. The spontaneous flux and the critical current modulation of the vortex states with the junction orientation are calculated by solving numerically the sine-Gordon equation. For SRO we shall assume three possible pairing states of two-dimensional order parameters, having line nodes within the RuO₂ plane, that break the time-reversal symmetry. The first two are the 2D, f -wave states proposed by Hasegawa *et al.*, [12] having $B_{1g} \times E_u$ and $B_{2g} \times E_u$ symmetry, respectively. The other one is called the nodal p -wave state and has been proposed by Dahm *et al.* [13], where the pairing potential has the form $\mathbf{d} = \Delta_0 \hat{\mathbf{z}}[\sin(k_x a) + i \sin(k_y a)]$. This pairing symmetry has nodes as in the $B_{2g} \times E_u$ case. Also we will consider two nodeless pairing states. One is the isotropic p -wave state and the other is the nodeless p -wave state initially proposed by Miyake and Narikiyo [14], both breaking the time-reversal symmetry. In addition we examine briefly several three-dimensional order parameters with horizontal lines of nodes.

For each pairing state we derive simple arguments that could be used to characterize it. For example the junction orientation where the a, b axes point towards the junction interface will give finite critical currents only for the isotropic p -wave, $B_{1g} \times E_u$ states and zeros for the other states. Furthermore the suppression of the critical currents of the nodal state $B_{1g} \times E_u$ near the nodes can be used to distinguish it from the nodeless isotropic p -wave state. Also the modulation of the Josephson critical current with the polar angle β , within the ac plane, will probe the horizontal nodes for hypothetical three-dimensional order-parameter symmetries. The rest of the paper is organized as follows. In Sec. II we discuss the Josephson effect between a superconductor breaking time-reversal symmetry and a conventional s -wave superconductor. In Sec. III the geometry of the corner junction is discussed. In Sec. IV we present the magnetic flux for the spontaneous vortex states. In Sec. V the modulation of the magnetic flux and the critical currents with the orientation are presented. In Sec. VI several three-dimensional order parameters are considered. In Sec.

VII the modulation of the vortex states with the magnetic field is discussed. In Sec. VIII a connection with the experiment is made. Finally, a summary and discussion are presented in the last section.

II. JOSEPHSON EFFECT BETWEEN SRO AND A CONVENTIONAL *S*-WAVE SUPERCONDUCTOR

We consider the junction shown in Fig. 1(a), between a superconductor *A* with a two-component order parameter n_A , and a superconductor *B* with order parameter n_B . The two superconductors are separated by an intermediate layer. The bulk order parameters n_A and n_B , near the interface, can be written as

$$n_A = \begin{cases} \tilde{n}_{A_x} e^{i\phi_{A_x}}, \\ \tilde{n}_{A_y} e^{i\phi_{A_y}} \end{cases} \quad (1)$$

and

$$n_B = \tilde{n}_B e^{i\phi_B}, \quad (2)$$

where ϕ_{A_x}, ϕ_{A_y} are the phases of the components of the order parameter n_A , and ϕ_B is the phase of the superconductor *B*. $\tilde{n}_{A_x}, \tilde{n}_{A_y}$ are the magnitudes of the components of the order parameter n_A . Then the supercurrent density can be written as

$$J = J_{BA_x} \sin(\phi_B - \phi_{A_x}) + J_{BA_y} \sin(\phi_B - \phi_{A_y}), \quad (3)$$

where

$$\begin{aligned} J_{BA_x} &\sim \tilde{n}_{A_x} \tilde{n}_B, \\ J_{BA_y} &\sim \tilde{n}_{A_y} \tilde{n}_B. \end{aligned} \quad (4)$$

We have to comment here that the coupling between a triplet and a singlet superconductor is forbidden by the orthogonality of the spin part of their wave functions. However, in our situation there exists a finite overlap due to spin-orbit coupling [15]. In the presence of spin-orbit coupling the Cooper pairs of different parities will be mixed at the interface

between the singlet and the triplet superconductor resulting in a direct Josephson coupling between them [16]. We define $\phi = \phi_B - \phi_{A_x}$ as the relative phase difference between two superconductors. We consider the case where the intrinsic phase difference within superconductor A is $\phi_{A_y} - \phi_{A_x} = \pi/2$. In this case the order parameter is complex and breaks the time-reversal symmetry. Then the supercurrent density can be written as: [17]

$$J(\phi) = \tilde{J}_c \sin(\phi + \phi_c), \quad (5)$$

with

$$\phi_c = \begin{cases} \tan^{-1} \frac{-J_{BA_y}}{J_{BA_x}} & J_{BA_x} > 0, \\ \pi + \tan^{-1} \frac{-J_{BA_y}}{J_{BA_x}} & J_{BA_x} < 0, \end{cases} \quad (6)$$

and

$$\tilde{J}_c = \sqrt{J_{BA_y}^2 + J_{BA_x}^2}. \quad (7)$$

We consider the following cases for the pairing state of SRO having line nodes.

(a) In the first 2D f -wave state $B_{1g} \times E_u$, the magnitudes of the order parameters \tilde{n}_{A_x} and \tilde{n}_{A_y} in Eq. (4) are defined as $\tilde{n}_{A_x} = \cos(2\alpha) \cos(\alpha)$, $\tilde{n}_{A_y} = \cos(2\alpha) \sin(\alpha)$. In these formulas α denotes the angle between the interface and the a axis of the crystal. This state has nodes at the same points as in the $d_{x^2-y^2}$ -wave case.

(b) For the second 2D f -wave state $B_{2g} \times E_u$, $\tilde{n}_{A_x} = \sin(2\alpha) \cos(\alpha)$, $\tilde{n}_{A_y} = \sin(2\alpha) \sin(\alpha)$. This state has nodes at $0, \pi/2, \pi$, and $3\pi/2$, and has also been studied by Graf and Balatsky [18].

(c) This is the case of a nodal p -wave superconductor, $\tilde{n}_{A_x} = 1/s_M \sin[\pi \cos(\alpha)]$, $\tilde{n}_{A_y} = 1/s_M \sin[\pi \sin(\alpha)]$. We use here the same normalization proposed by Dahm *et al.*, [13] $s_M = \sqrt{2} \sin(\pi/\sqrt{2}) = 1.125$, where the Fermi wave vector is chosen as $k_{Fa} = \pi$, in order to have a node of the order parameter in the Fermi surface. This state has nodes as in the $B_{2g} \times E_u$ state. The corresponding nodeless form was initially proposed by Miyake, and Narikiyo [14] and will be considered as a separate case. Also we will examine the following two pairing symmetries, which are nodeless

d) In the case of a nodeless p -wave superconductor, proposed by Miyake and Narikiyo [14] $\tilde{n}_{A_x} = 1/s_M \sin[R\pi \cos(\alpha)]$, $\tilde{n}_{A_y} = 1/s_M \sin[R\pi \sin(\alpha)]$, $s_M = \sqrt{2} \sin(\pi/\sqrt{2}) = 1.125$, and $R = 0.9$. This state does not have nodes.

e) In the isotropic p -wave case, $\tilde{n}_{A_x} = \cos(\alpha)$, $\tilde{n}_{A_y} = \sin(\alpha)$. This pairing state does not have nodes either.

III. THE JUNCTION GEOMETRY

We consider the corner junction shown in Fig. 1(b) between a triplet superconductor breaking the time-reversal symmetry and an s -wave superconductor. In the following the Josephson coupling is restricted in the ab plane since we assume 2D order parameters. If the angle of the a axis with the interface in the x direction is α , then the corresponding angle in the y direction will be $\pi/2 - \alpha$. Using this constraint we map the two segments of this corner junction, each of length $L/2$, into a one-dimensional axis shown in Fig. 1(c). In this case the two-dimensional junction can be considered as being made of two one-dimensional junctions described in Sec. II connected in parallel. The characteristic phases of the two parts of the one-dimensional junction ϕ_{c1} and ϕ_{c2} depend upon the angle α . We call this junction frustrated since the two segments have different characteristic phases ϕ_{c1} and ϕ_{c2} . The fabrication details of corner junctions or SQUID's, between sample faces at different angles, can be found in Refs. [19] and [20].

The superconducting phase difference ϕ across the junction is then the solution of the sine-Gordon equation

$$\frac{d^2\phi(x)}{dx^2} = \tilde{J}_c \sin[\phi(x) + \phi_c(x)] - I^{ov}, \quad (8)$$

with the boundary conditions

$$\frac{d\phi}{dx}\Big|_{x=0,L} = H, \quad (9)$$

where $\phi_c(x) = \phi_{c1}(\phi_{c2})$ in the left (right) part of the junction, and I^{ov} is the bias current in

the overlap geometry. The length x is scaled in units of the Josephson penetration depth given by

$$\lambda_J = \sqrt{\frac{\hbar c^2}{8\pi e d J_{c0}}},$$

where d is the sum of the s -wave, and mixed wave, in-plane penetration depths plus the thickness of the insulator layer. The different solutions obtained from Eq. (8) are classified with their magnetic-flux content

$$\Phi = \frac{1}{2\pi}(\phi_R - \phi_L), \quad (10)$$

where $\phi_{R(L)}$ is the value of ϕ at the right (left) edge of the junction, in units of the flux quantum $\Phi_0 = hc/2e$.

To check the stability of solutions we consider small perturbations $u(x, t) = u(x)e^{st}$ on the static solution $\phi(x)$, and linearize the time-dependent sine-Gordon (s-G) equation to obtain

$$\frac{d^2 v(x)}{dx^2} + \tilde{J}_c \cos[\phi(x) + \phi_c(x)]v(x) = \lambda v(x), \quad (11)$$

where $\lambda = -s^2$, with the boundary conditions

$$\frac{dv}{dx}\Big|_{x=0,L} = 0. \quad (12)$$

It is seen that if the eigenvalue equation has a negative eigenvalue the static solution $\phi(x)$ is unstable.

IV. SPONTANEOUS VORTEX STATES

First let us consider the case where the two one-dimensional junctions between a triplet superconductor breaking the time-reversal symmetry and an s -wave superconductor, each of length $L/2$, described in Sec. II, are uncoupled. Then for $0 < x < L/2$ the stable solutions for the s-G equation are $\phi(x) = -\phi_{c1} + 2n_1\pi$, where $n_1 = 0, \pm 1, \pm 2, \dots$, while for $L/2 < x < L$ the stable solutions for the s-G equation are $\phi(x) = -\phi_{c2} + 2n_2\pi$, where $n_2 = 0, \pm 1, \pm 2, \dots$,

and ϕ_{c1} , ϕ_{c2} are the relative phases in each part of the junction due to different orientations. When the frustrated junction is formed, and we consider the above junctions in parallel, the phase ϕ is forced to change around $x = L/2$ to connect these stable solutions. This variation of the phase ϕ along the junction describes the Josephson vortices. The flux content of these states (in units of Φ_0) is [21]

$$\Phi = [\phi(L) - \phi(0)]/2\pi = (-\phi_{c2} + \phi_{c1} + 2n\pi)/2\pi, \quad (13)$$

where the n value ($n = n_1 - n_2 = 0, \pm 1, \pm 2, \dots$) distinguishes between solutions with different flux content. We will concentrate on solutions called modes with minimum flux content, i.e., $n = 0, 1, -1$. Their magnetic flux in terms of ϕ_{c1}, ϕ_{c2} is shown in Table I. Generally the flux content is fractional, i.e., is neither integer nor half-integer, as a consequence of the broken time-reversal symmetry of the problem.

V. SPONTANEOUS MAGNETIC FLUX AND CRITICAL CURRENTS

In this section we will consider the magnetic flux and critical current modulation with the azimuthal angle α , for the various two-dimensional pairing states for the SRO. In general the flux quantization and the critical currents are influenced by the nodal structure of the order parameter. The critical current I_c^{ov} which depends mainly on the magnitude of the order parameter vanishes at the nodes of the order parameter. The magnetic flux is determined from ϕ_{c1}, ϕ_{c2} , and has almost the same structure in the isotropic p -wave, $B_{1g} \times E_u$ and $B_{2g} \times E_u$ pairing states, while it is different in the nodal p -wave and the nodeless p -wave cases.

A. Isotropic p wave

For the isotropic p -wave case we present in Fig. 2(a) the variation of ϕ_{c1}, ϕ_{c2} , with the interface orientation angle α . The magnetic flux can be calculated analytically for the spontaneous vortex states $0, -1, 1$. The corresponding expressions are seen in Table II. The

spontaneous magnetic flux as a function of the angle α is presented in Fig. 2(b). At $\alpha = 0$ we have the existence of three possible spontaneous vortex states. As we change the angle α , the magnetic flux changes, keeping the distance between the modes at a constant value equal to a single flux quantum. The modes for $\alpha = 0$ are displaced to quadratic values [i.e., $(1/4 + n)\Phi_0$] of the magnetic flux in contrast to the s -wave case where the flux is quantized in integer values $0, -1, 1$ [22].

In particular the vortex solution in the $n = 0$ mode (solid line) contains $1/4$ of a fluxon for $\alpha = 0$, and as we increase the angle α towards $\pi/4$ it continuously reduces its flux, i.e., it becomes flat exactly at $\alpha = \pi/4$ and then it reverses its sign and becomes an antivortex with exactly opposite flux content at $\alpha = \pi/2$ from that at $\alpha = 0$. In addition we have plotted in Fig. 3(a) the phase distributions for the mode $n = 0$ in different orientations $\alpha = 0, \pi/4, \pi/2$. The transition from the vortex to the antivortex mode as the orientation changes is clearly seen in this figure. Note that the solutions in this mode remain stable for all junction orientations. This is seen in Fig. 2(c) where we plot the lowest eigenvalue (λ_1) of the linearized eigenvalue problem as a function of the angle α . We see that $\lambda_1 > 0$, denoting stability for all values of the angle α in this mode.

Let us now examine the solution in the $n = -1$ mode [dashed line in Fig. 2(b)]. We see that at $\alpha = 0$ it has negative flux, equal to -0.75 , and is stable. As we increase the angle α it decreases its flux to a full antfluxon when the orientation is $\pi/4$ and then to flux of -1.25 when α reaches $\pi/2$. As seen in Fig. 2(c) this solution becomes unstable at $\alpha = \pi/4$ where a full antfluxon enters the junction. The phase distribution at this point is seen in Fig. 3(b) (dotted line).

Finally the solution in the $n = 1$ mode [long-dashed line in Fig. 2(b)] contains 1.25 in flux at $\alpha = 0$ and is clearly unstable. It becomes stable at $\alpha = \pi/4$ [see Fig. 2(c) (long-dashed line)], where a full fluxon enters the junction, as seen in Fig. 3(c) (dotted line). At $\alpha = \pi/2$ it contains 0.75 in flux.

In Fig. 2(d) we plot the overlap critical current per unit length I_c^{ov} as a function of the angle α , at $H = 0$, for the $n = 0, -1, 1$ -mode solutions. The Josephson critical current

density is kept constant with the orientation $\tilde{J}_c = 1$. Let us consider the situation where the junction contains a solution in the mode $n = 0$, at $\alpha = 0$, when the net current is maximum. The spatial variation of ϕ is described by a fractional vortex displaced from the corresponding distribution at zero current which is around $\pi/4$ [see Fig. 3(a)]. The current-density distribution as seen in Fig. 4(a) (solid line) corresponds to a positive fluxon, and at the maximum current is flat, close to unity, and has a small variation around the junction center giving rise to the large value of the net current, seen in Fig. 2(d). At $\alpha = \pi/4$ the flat phase distribution corresponding to the $n = 0$ solution seen in Fig. 3(a) at zero current is displaced towards the value $3\pi/4$ at the maximum current. The current-density distribution as seen in Fig. 4(a) (dotted line) is flat, giving a net current equal to 1 which is the maximum value over the range $0 < \alpha < \pi/2$.

For the -1 solution at $\alpha = 0$ the phase represents an antifluxon which is being displaced at the maximum current from the corresponding distribution at zero current seen in Fig. 3(b). The corresponding current density represents an antifluxon, and has a characteristic variation along the junction, taking positive and negative values, as seen in Fig. 4(b) (solid line), so that the net current is suppressed compared to the 0 mode. At $\alpha = \pi/4$ just one antifluxon enters the junction and the current distribution is symmetric around $x = L/2$, as seen in Fig. 4(b) (dotted line), leading to zero total current at this angle.

The critical current I_c^{ov} for the 0 mode is finite for each orientation α due to the nodeless form of the order parameter. This is in marked contrast to what we see in the singlet pairing states that describe the high- T_c cuprates where the critical current I_c^{ov} for the different modes is suppressed near $\alpha = \pi/4$ following a similar variation to the Josephson critical current density $\tilde{J}_c(\alpha)$ [23]. Also the fractional values of the magnetic flux are originated from the two-component order parameter that breaks the time-reversal symmetry.

B. $B_{1g} \times E_u$

In the $B_{1g} \times E_u$ -wave pairing state the ϕ_{c1}, ϕ_{c2} and also the magnetic flux seen in Fig. 5(a) and Fig. 5(b), respectively, have the same form as in the isotropic p -wave case. This happens because the relative phase ϕ_c in Eq. (6) depends on the ratio of the real and imaginary parts of the order-parameter magnitude in superconductor SRO. The B_{1g} component $\cos 2\alpha$ multiplies both parts and is canceled out. On the contrary only the B_{1g} part of the order parameter contributes to the Josephson critical current density \tilde{J}_c , which varies as $|\cos(2\alpha)|$ as seen in Fig. 5(a) (dashed line), while the E_u part is canceled. It has nodes at $\alpha = \pm\pi/4$. For this reason we choose the interval $-\pi/4 < \alpha < \pi/4$ to study the $B_{1g} \times E_u$ pairing state.

For $\alpha = 0$ the mode $n = 0$ contains negative magnetic flux of -0.25 as seen in Fig. 5(b), the mode 1 contains positive magnetic flux equal to 0.75 and is stable, while the mode -1 has -1.25 in flux and is unstable. The variation of the phase of the vortex solutions at zero current and the corresponding current density at maximum current for $\alpha = 0$ are seen in Fig. 6. Differently from the isotropic p -wave case, the mode 0 with negative magnetic flux corresponds to the highest critical current.

Close to $\pm\pi/4$ the variation of the magnetic flux for the modes $0, -1, 1$ is influenced from the suppression of the \tilde{J}_c which goes to zero at $\pm\pi/4$ and the magnetic flux acquires some curvature at these points as seen in Fig. 5(b). Due to this abrupt variation the numerical procedure to follow modes $-1, 1$ stops at the point where the flux changes more rapidly. This is the reason why the magnetic flux for the modes $-1, 1$ does not reach the nodes of the \tilde{J}_c at $\alpha = \pm\pi/4$.

Also the critical currents are influenced by the \tilde{J}_c . The critical current for the mode 0 vanishes at $\alpha = \pm\pi/4$ where the order parameter has nodes. Also the maximum of the critical current tends to move towards $\alpha = 0$ where \tilde{J}_c has its maximum value. On the other hand the phase prefers the orientation $\alpha = -\pi/4$ where it is flat. These two competitive factors shift the maximum current for $n = 0$ to the left of $\alpha = 0$. The critical currents for the other two modes are suppressed close to $\alpha = \pm\pi/4$ where the order parameter has

nodes. In particular for mode 1 the magnetic flux is smaller compared to mode -1 and as a consequence the critical current is higher. In the interval we study, mode -1 is unstable while modes $1, 0$ are stable as seen in Fig. 5(c), where the lowest eigenvalue λ_1 versus α is plotted.

C. $B_{2g} \times E_u$

In the $B_{2g} \times E_u$ case the ϕ_{c1}, ϕ_{c2} seen in Fig. 7(a) have the same form as in the isotropic p wave case. Here the B_{2g} factor of the order parameter $\sin 2\alpha$ is canceled out in the calculation of the relative phase $\phi_c(x)$. The B_{2g} part of the order parameter influences the Josephson critical current \tilde{J}_c , which varies as $|\sin(2\alpha)|$ as seen in Fig. 7(a) (dashed line) and has nodes at $0, \pi/2$. Due to this form of the \tilde{J}_c we have nodes at the critical current I_c^{ov} versus α at the points $0, \pi/2$, as seen in Fig. 7(d). The modes $1, -1$ have zero critical current at the angle $\alpha = \pi/4$ where a full fluxon or antifluxon enters into the junction. In addition they become zero close to 0 or $\pi/2$ due to the vanishing of \tilde{J}_c at these angles. Note that close to 0 or $\pi/2$ the form of \tilde{J}_c influences also the magnetic flux at zero current which acquires a small curvature at these points. The mode 0 has its maximum close to $\alpha = 0$ in the $B_{1g} \times E_u$ state while in $B_{2g} \times E_u$ the critical current at $\alpha = 0$ becomes zero. In the isotropic p -wave case the critical current is finite at $\alpha = 0$ since the order parameter for this state is nodeless.

D. Nodal p wave

For the nodal p -wave case the ϕ_{c1}, ϕ_{c2} are interchanged compared to the isotropic p -wave and $B_{1g} \times E_u$ cases and also their linear form is lost. As a result the slope of the magnetic flux versus α seen in Fig. 8(b) has changed from negative in the isotropic p -wave and $B_{2g} \times E_u$ cases to positive here. Now mode 1 is stable in the interval $0 < \alpha < \pi/4$ and mode -1 is stable in the interval $\pi/4 < \alpha < \pi/2$, contrary to the isotropic p -wave case as seen in Fig. 8(c). The Josephson critical current density \tilde{J}_c has the same nodal form as in the $B_{2g} \times E_u$ case, with nodes at $0, \pi/2$, as seen in Fig. 8(a), since the nodal form of the order

parameter is the same. The critical current for mode 0 versus α follows the same form as in the $B_{2g} \times E_u$ case and it is zero at $0, \pi/2$ and maximum at $\alpha = \pi/4$, where the phase is uniform. Also the variation of the flux versus α seen in Fig. 8(b) is quite close to zero for mode 0, and as a consequence the I_c^{ov} vs α for mode 0 is more broadened compared to the corresponding mode in the $B_{2g} \times E_u$ case. The mode $-1(1)$ becomes zero at $\alpha = \pi/4$ where a full antfluxon (fluxon) enters the junction. For $\alpha < \pi/4$, mode 1 has less magnetic flux in absolute value than does mode -1 and its critical current I_c^{ov} is higher. On the other hand for $\alpha > \pi/4$, mode 1 has more magnetic flux in absolute value than does mode -1 and its critical current I_c^{ov} is lower. Note that modes $-1, 1$ stop abruptly at the angle where the variation of the flux is more abrupt

E. Nodeless p wave

For the nodeless p -wave case the variation of ϕ_{c1}, ϕ_{c2} is more complex. It is similar to the nodal p -wave case except at values close to $0, \pi/2$ where it changes slope. As a result the magnetic flux versus α varies more closely to integer values and is almost flat as seen in Fig. 9(b). Also within the interval $0 < \alpha < \pi/2$ modes $-1, 1$ change from stable to unstable for more than one time as seen in Fig. 9(c) while mode 0 is stable for all values of α . The \tilde{J}_c has a nodeless form as seen in Fig. 9(a), i.e., it has no zero values. As a consequence the critical current for mode 0 is finite over the angles α and has its maximum values at $\alpha = \pi/4$ where the phase is uniform. At this point a full fluxon or antfluxon enters the junction and the critical current for modes $-1, 1$ is zero. Also the magnetic flux for modes $-1, 1$ varies close to values $-1, 1$ and as a consequence their critical currents are almost coincident.

VI. 3D ORDER PARAMETERS WITH HORIZONTAL LINES OF NODES

In the preceding sections we considered purely two-dimensional order parameters. In this section we consider the case where the order parameter is three dimensional. Recent measurement of thermal conductivity under a rotating in-plane magnetic field by Izawa *et*

al. [5] has shown a fourfold pattern with a minimum when $H \parallel [110]$ and suggests that the nodes of the gap are on the line with $k_z = \text{const}$ as discussed in Ref. [12]. So the question arises also whether the results obtained in the present paper remain valid for such pairings.

Several three-dimensional order parameters have been proposed in the literature: Hasegawa *et al.* [12] have proposed the pairing states with order parameter $\mathbf{d} = \Delta_0 \hat{\mathbf{z}}(k_x + ik_y) \cos(ck_z)$ and $\mathbf{d} = \Delta_0 \hat{\mathbf{z}}[\sin(ak_x/2) + i \sin(a/2)] \cos(ck_z/2)$ with c being the lattice constant along the c axis. These states have horizontal lines of nodes at $k_z = \pm\pi/2c$ and $k_z = \pm\pi/c$, respectively, and break the time-reversal symmetry. Also Won and Maki [24] have proposed an f -wave model with a superconducting order parameter $\mathbf{d} = \Delta_0 \hat{\mathbf{z}}(k_x + ik_y)^2 k_z$. This state has horizontal lines of nodes where the basal plane $k_z = 0$ intersects the Fermi surface.

In all the above pairing states the Josephson current within the ab plane is canceled, since the order parameter changes sign in the k_z direction symmetrically around zero. However it is possible to have finite Josephson current when the Fermi surface is not exactly cylindrical but is corrugated as observed by the angle dependence of the de Haas-van Alphen effect [25]. In that case the cancellation would not be complete. Another possibility to have finite Josephson current within the ab plane is to have a three-dimensional order parameter that is mixed with a two-dimensional one as suggested also in Ref. [12]. Then for the Josephson effect within the ab plane, discussed in preceding sections, the quasiparticles will experience an effective order parameter that is quasi-two-dimensional and the modulation of the critical current and magnetic flux with the misorientation angle within the ab plane will show the nodal profile of the order parameter within the ab plane discussed previously.

In an alternative geometry, the modulation of the critical current and spontaneous flux with the polar misorientation angle within the ac plane, i.e., when the azimuthal angle is set to zero $\alpha = 0$, would reveal the angular anisotropy of the order parameter along the c axis. In that case the effective order parameter felt by the quasiparticles is two dimensional. Moreover for that orientation the two-component order parameter is reduced to a one-component one which has a sign change but does not break time-reversal symmetry.

For example we consider the three-dimensional order parameter $\mathbf{d} = \Delta_0 \hat{\mathbf{z}}(k_x +$

$ik_y) \cos(ck_z)$. For a spherical Fermi surface and $\alpha = 0$, it is reduced to the two-dimensional order parameter $\mathbf{d} = \Delta_0 \hat{\mathbf{z}} \sin \beta \cos(\pi \cos \beta)$. We plot in Fig. 10(a) the order parameter for adjacent crystal edges versus the polar angle β . It is seen that the order parameter changes sign, in a restricted angle regime, at adjacent faces of the crystal. Also the characteristic phases ϕ_{c1}, ϕ_{c2} differ by π as seen in Fig. 10(b). That would, for example, lead to half-integer spontaneous flux states. Note that the Josephson critical current densities as seen in Fig. 10(c) are not equal for adjacent junction edges. However the asymmetry in the current densities will not affect that spontaneous flux. The modulation of the current with the polar angle within the ac plane will be highly anisotropic for the three-dimensional order parameters. It will be suppressed for $ck_z = \pi/2$ for the pairing state $\Delta \propto \cos ck_z$.

Since all states considered here have $\mathbf{d} \parallel \hat{\mathbf{z}}$ the Josephson current along the c axis between the singlet and triplet superconductors is not allowed [16]. In fact the spin-orbit coupling strength of the triplet superconductor would give rise to the orientational dependent Josephson coupling between the SRO and the conventional s -wave superconductor which completely vanishes along the c axis. However the Josephson coupling is possible when the \mathbf{d} vector is not exactly parallel to the current. In that case we restrict to the corner junction in the ac plane where the c axis is tilted within the ac plane for certain polar angle. For the pairing state $\Delta \propto k_z$ the singlet-superconductor/triplet-superconductor/singlet-superconductor junction along a direction slightly different from the c axis can be used to probe the pairing symmetry from the sign change of the Josephson current at opposite faces of the junction [26].

VII. MAGNETIC FIELD

We now examine the influence of the magnetic field on the spontaneous vortices, for the ab -plane Josephson effect, for fixed junction orientation $\alpha = 0$, where most experiments on corner junctions have been performed. The critical current is finite, at $\alpha = 0$ for the pairing states isotropic p wave and $B_{1g} \times E_u$, while it is zero or very suppressed for the other pairing

states. Hence we will restrict ourselves only to the isotropic p wave and $B_{1g} \times E_u$ at $\alpha = 0$ in this section. The modes extend to a large interval of the magnetic field, which is almost the same. The instability at the extremum values of the magnetic field is due to the interaction of the flux entered from the edges with the intrinsic flux. The separation of the modes in magnetic flux is kept constantly equal to Φ_0 as in the s -wave case, but is displaced compared to the s -wave case by an amount that is equal to the intrinsic flux.

We plot in Fig. 11(a) the overlap critical current I_c^{ov} versus the magnetic field H , for a junction with length $L = 10$, for angle $\alpha = 0$, and for the isotropic p -wave case. The mode 0, at $H = 0$, contains positive flux $\Phi = 0.25$ and has greater critical current than mode -1 , which at $H = 0$ contains negative magnetic flux and is equal to -0.75 . So the mode with positive magnetic flux corresponds to the highest critical current. The maximum I_c^{ov} for mode 0 occurs to the right of $H = 0$. Note that the displacement of modes 0, -1 , 1 in Φ from their positions in the s -wave case is small and thus the I_c^{ov} vs H diagram is similar to the s -wave case.

In Figs. 12(a) and 12(b), the overlap critical current I_c^{ov} versus the magnetic field H and the spontaneous flux vs magnetic field is plotted for the $B_{1g} \times E_u$ case. The mode 0, at $H = 0$, contains negative flux $\Phi = -0.25$ and has greater critical current than mode 1, which at $H = 0$ contains positive magnetic flux and is equal to 0.75 . So differently from the isotropic p -wave case, the mode with negative magnetic flux corresponds to the highest critical current.

For the rest of the pairing states the junction orientation $\alpha = 0$ gives zero or relatively small values for the Josephson critical current density $J_c(\alpha)$, which means that the critical current the junction can carry will be zero or very suppressed compared to the previous cases. For the ac -plane Josephson effect for three-dimensional order parameters it is possible to have a sign change of the order parameter at adjacent faces of the corner junction that would, for example lead to an anomalous Fraunhofer pattern with "dip" at zero magnetic field. The asymmetry in the Josephson critical current densities will only cause the "dip" to be shallow and will maintain the symmetry of the pattern.

VIII. EXPERIMENTAL RELEVANCE

For the ab -plane Josephson effect for two-dimensional order parameters, the measurement of the magnetic interference pattern at $\alpha = 0$ where the a and b crystallographic axes are perpendicular to the junction's faces will not give any finite value for the critical current I_c^{ov} for the pairing states $B_{2g} \times E_u$ or the nodal p wave since the value $\alpha = 0$ is a node of the order parameter for these symmetries. For the nodeless p -wave case the Josephson critical current density is small at $\alpha = 0$ and so is the critical current. So the observation of finite critical current I_c^{ov} in corner junctions at $\alpha = 0$ would be an indication for isotropic p -wave or $B_{1g} \times E_u$ pairing states where the value $\alpha = 0$ is not a node. Furthermore the suppression of the critical currents of the nodal state $B_{1g} \times E_u$ near the nodes, i.e., at $\alpha = \pm\pi/4$, can be used to distinguish it from the nodeless isotropic p -wave state, for which the critical current for no-flux mode 0 does not become zero.

On the other hand for the ac -plane tunneling, the orientation where $ck_z = \pi/2$ will suppress the Josephson critical current for the pairing state $\Delta \propto \cos ck_z$ since it is a node for the order parameter. Also the singlet/triplet/singlet junction along the direction slightly different from the c axis will probe the pairing state $\Delta \propto k_z$ from the sign change of the Josephson current at opposite sides of the junction.

Another experiment that we propose here to discriminate between the candidate's pairing states consists of a SQUID between a Sr_2RuO_4 thin film patterned into a circle with a series of Nb-Au- Sr_2RuO_4 edge junctions spaced at a fixed angle step. The tunneling directions can be defined lithographically and patterned by ion milling of a c -axis-oriented film to study the ab -plane Josephson effect or a b -axis-oriented film to study the ac -plane Josephson effect. The measurement of the critical current versus the angle α , which mainly probes the magnitude of the order parameter, is expected to show large anisotropy with the angle α . An analogous experiment has already been performed in the SQUID geometry for $\text{YBa}_2\text{Cu}_3\text{O}_7$ thin films [20].

A number of complicating factors are involved in the interpretation of the experiments

with corner junctions that could modify the anticipated results. These include the asymmetry in the Josephson critical current densities, the flux trapping, and the sample geometry. Also the study of the direction-dependent Josephson effect will be influenced by the roughness of the interface due to the existence of Ru lamellas, and also by the difficulty in cleaning and polishing a crystal at angles different than 0 and $\pi/2$. However these effects are not sufficiently large enough to change the qualitative picture of the experiments.

IX. CONCLUSIONS

We followed the modulation of the vortices that are spontaneously formed in a corner junction between a triplet superconductor breaking time-reversal symmetry and an *s*-wave superconductor with the junction orientation angle. The nodal structure of the order parameter is reflected in the Josephson critical current density, and influences the critical current versus α diagram and the magnetic flux of the spontaneous vortex states that are formed at the corner junction. The critical current vanishes at the angles where the order parameter has nodes. In addition it becomes zero at the angles where a full fluxon or antfluxon enters the junction. For the nodeless pairing state mode 0 does not vanish, and has the nodal profile of the corresponding order parameter. The presence of spontaneous magnetic flux can be used to distinguish between different symmetry states.

The external magnetic field for the junction orientation $\alpha = 0$ where the *a* axis points towards the junction edge will only influence the states in which their order parameter is finite at $\alpha = 0$, i.e., isotropic *p* wave and $B_{1g} \times E_u$. The critical current and the effect of the magnetic field will be zero or very suppressed for the other cases. For three-dimensional order parameters the Josephson critical current modulation, which mainly probes the magnitude of the order parameter with the polar angle, is expected to be highly anisotropic for the *ac*-plane Josephson effect.

In corner junctions with broken time-reversal symmetry, the spontaneous flux and the magnetic interference pattern, even in the short junction limit, are influenced by the mag-

nitude of the order parameter and also the difference in the intrinsic phases ϕ_{c1} and ϕ_{c2} , at adjacent junction edges. This difference uniquely characterizes the pairing symmetry and can be used without any ambiguity to probe anisotropic pairing states with sign change of the order parameter between orthogonal directions in k space.

REFERENCES

- [1] Y. Maeno, H. Hashimoto, K. Yoshida, S. Nishizaki, T. Fujita, G.J. Bednorz and F. Lichtenberg, *Nature (London)* **372**, 532 (1994).
- [2] K. Ishida, H. Mukuda, Y. Kitaoka, K. Asayama, Z.Q. Mao, Y. Mori, and Y. Maeno, *Nature (London)* **396**, 653 (1998).
- [3] G.M. Luke, Y. Fukamoto, K.M. Kojima, M.L. Larkin, J. Merrin, B. Nachumi, Y.J. Uemura, Y. Maeno, Z.Q. Mao, Y. Mori, H. Nakamura, and M. Sgrist, *Nature (London)* **394**, 558 (1998).
- [4] S. Nishizaki, Y. Maeno, and Z. Mao, *J. Phys. Soc. Jpn.* **69**, 572 (2000).
- [5] K. Izawa, H. Takahashi, H. Yamaguchi, Yuji Matsuda, M. Suzuki, T. Sasaki, T. Fukase, Y. Yoshida, R. Settai, and Y. Onuki, *Phys. Rev. Lett.* **86**, 2653 (2001).
- [6] A.P. Mackenzie, R.K.W. Haselwimmer, A.W. Tyler, G.G. Lonzarich, Y. Mori, S. Nishizaki, and Y. Maeno, *Phys. Rev. Lett.* **80**, 161 (1998).
- [7] N. Stefanakis, *J. Phys.: Condens. Matter* **13**, 3643 (2001).
- [8] N. Stefanakis, cond-mat/0201062 (unpublished).
- [9] R. Jin, Yu. Zadorozhny, Y. Liu, D.G. Schlom, Y. Mori, and Y. Maeno, *Phys. Rev. B* **59**, 4433 (2000).
- [10] M. Yamashiro, Y. Tanaka, and S. Kashiwaya, *J. Phys. Soc. Jpn.* **67**, 3364 (1998).
- [11] R. Jin, Y. Liu, Z.Q. Mao, and Y. Maeno, *Europhys. Lett.* **51**, 341 (2000).
- [12] Y. Hasegawa, K. Machida, and M. Ozaki, *J. Phys. Soc. Jpn.* **69**, 336 (2000).
- [13] T. Dahm, H. Won, and K. Maki, cond-mat/0006301 (unpublished).
- [14] K. Miyake and O. Narikiyo, *Phys. Rev. Lett.* **83**, 1423 (1999).
- [15] C. Honerkamp and M. Sgrist, *Progr. Theor. Phys.* **100**, 53 (1998).

- [16] V.B. Geshkenbein and A.I. Larkin, Pis'ma Zh. Eksp. Teor. Fiz. **43**, 306 (1986) [JETP Lett. **43**, 395 (1986)].
- [17] J.-X. Zhu, W. Kim, and C.S. Ting, Phys. Rev. B **58**, 6455 (1998).
- [18] M.J. Graf and A.V. Balatsky, Phys. Rev. B **62**, 9697 (2000).
- [19] D.J. van Harlingen, Rev. Mod. Phys. **67**, 515 (1995).
- [20] D.J. van Harlingen, J.E. Hilliard, B.L.T. Plourde, and B.D. Yanoff, Physica C **317-318**, 410 (1999).
- [21] M. Sigrist, Prog. Theor. Phys. **99**, 899 (1998).
- [22] C.S. Owen and D.J. Scalapino, Phys. Rev. **164**, 538 (1967).
- [23] Y. Tanaka and S. Kashiwaya, Phys. Rev. B **56**, 892 (1997).
- [24] H. Won and K. Maki, Europhys. Lett. **52**, 427 (2000).
- [25] Y. Yoshida, R. Settai, Y. Onuki, H. Takei, K. Betsuyaku, and H. Harima, J. Phys. Soc. Jpn. **67**, 1677 (1998).
- [26] V.B. Geshkenbein, A.I. Larkin, and A. Barone, Phys. Rev. B **36**, 235 (1987).

TABLE I. The magnetic flux (Φ) in terms of ϕ_{c1} , ϕ_{c2} for the spontaneous solutions that exist in a corner junction between a triplet superconductor with time-reversal broken symmetry and an s -wave superconductor (ϕ_{c1}, ϕ_{c2} is the extra phase difference in the two edges of the corner junction due to the different orientations, of the a axis of the triplet superconductor). We present only the minimum flux states $n = 0, -1, 1$.

Vortex state	Magnetic flux (Φ)
0	$(-\phi_{c2} + \phi_{c1})/2\pi$
1	$(-\phi_{c2} + \phi_{c1} + 2\pi)/2\pi$
-1	$(-\phi_{c2} + \phi_{c1} - 2\pi)/2\pi$

TABLE II. The magnetic flux (Φ) in terms of α for the spontaneous vortex states that exist in a corner junction between a triplet superconductor with isotropic p -wave symmetry and an s -wave superconductor.

Vortex state	Magnetic flux (Φ)
0	$0.25 - \alpha/\pi$
1	$1.25 - \alpha/\pi$
-1	$-0.75 - \alpha/\pi$

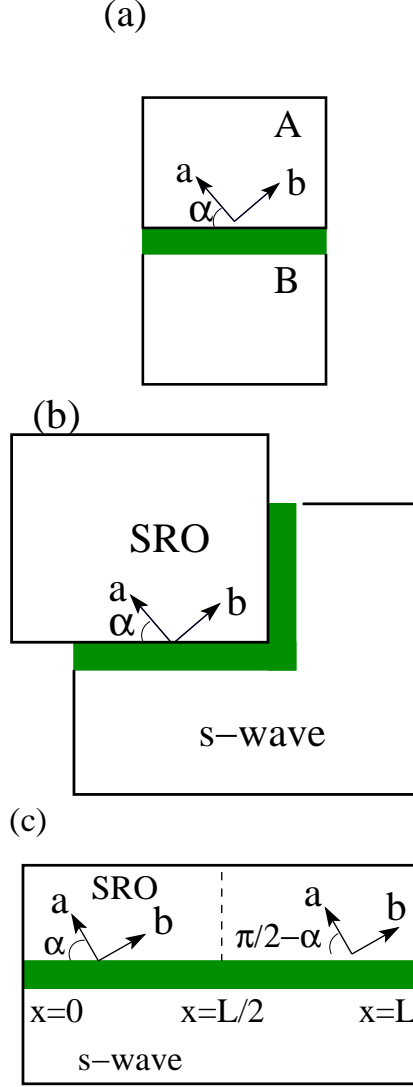


FIG. 1. (a) A single Josephson junction between a triplet superconductor A with broken time-reversal pairing symmetry and B , with s -wave symmetry. The angle between the crystalline a axis of A and the junction interface is α . (b) The geometry of the corner junction between superconductors SRO and s wave. (c) The mapping of the corner junction geometry into the one-dimensional axis of length L . For $0 < x < L/2$ the angle between the a axis and the interface is α while for $L/2 < x < L$ the corresponding angle is $\pi/2 - \alpha$.

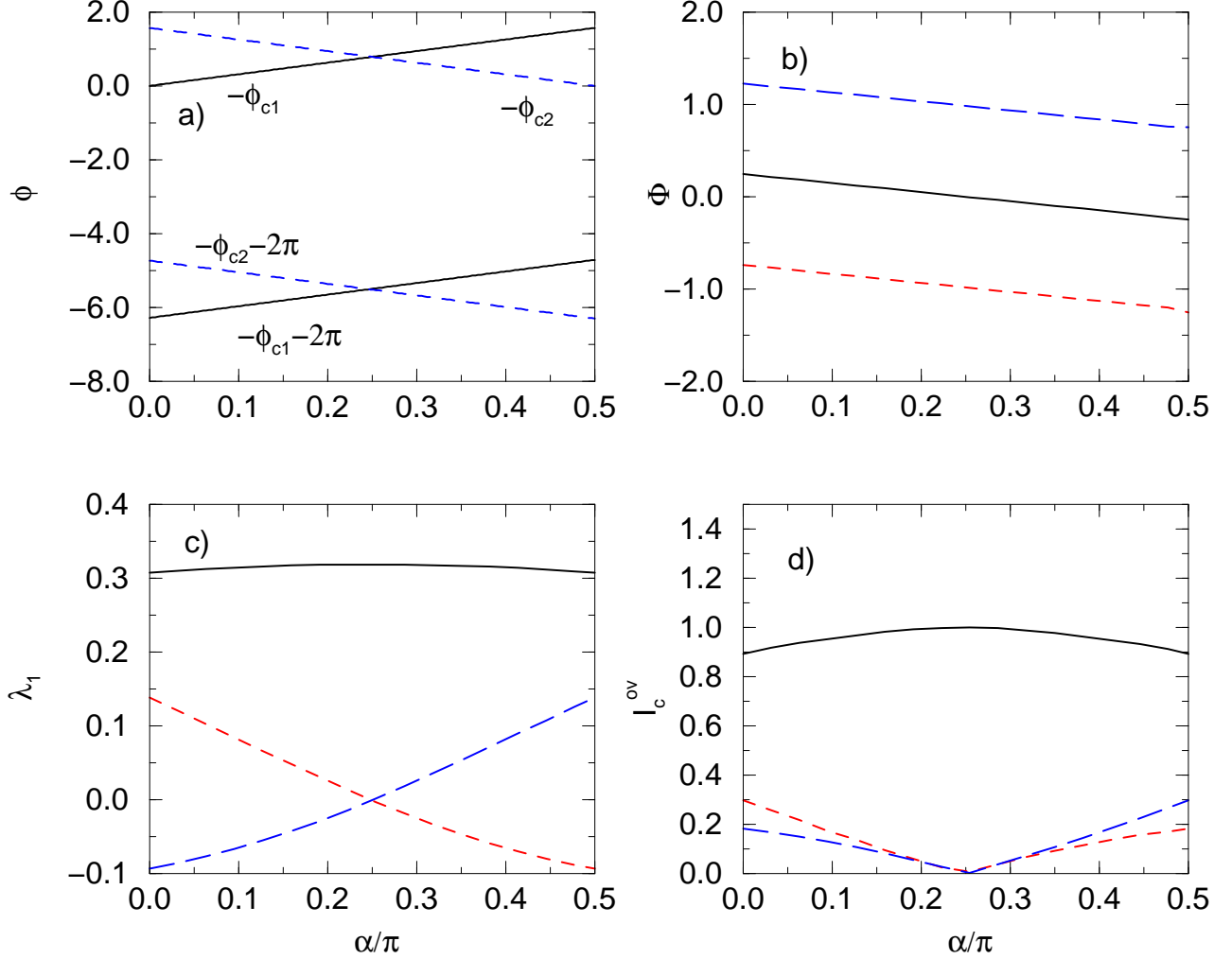


FIG. 2. (a) The variation of ϕ_{c1} , ϕ_{c2} with the angle α . For each value of α there exist three vortex solutions. (b) The spontaneous magnetic flux Φ as a function of the angle α , for the 0, -1, 1 mode solutions as solid, dashed, and long-dashed lines respectively. (c) The lowest eigenvalue λ_1 as a function of the angle α , for the 0, -1, 1 mode solutions. (d) Overlap critical current density I_c^{ov} versus the angle α for a junction of length $L = 10$. The pairing symmetry of the triplet superconductor is isotropic p wave.

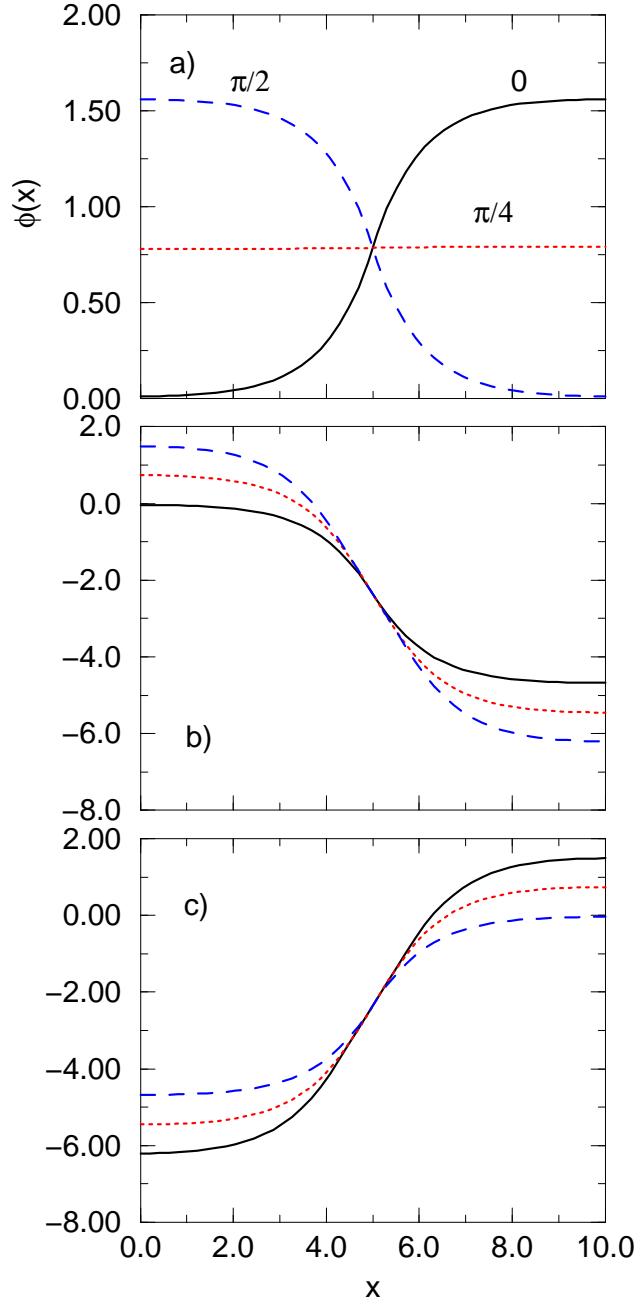


FIG. 3. The phase distribution of the vortex solutions (a) $n = 0$, (b) $n = -1$, and (c) $n = 1$, at $\alpha = 0, \pi/4, \pi/2$; for a corner junction of isotropic p -wave and s -wave superconductors, with length $L = 10$, and zero overlap external current $I^{ov} = 0$.

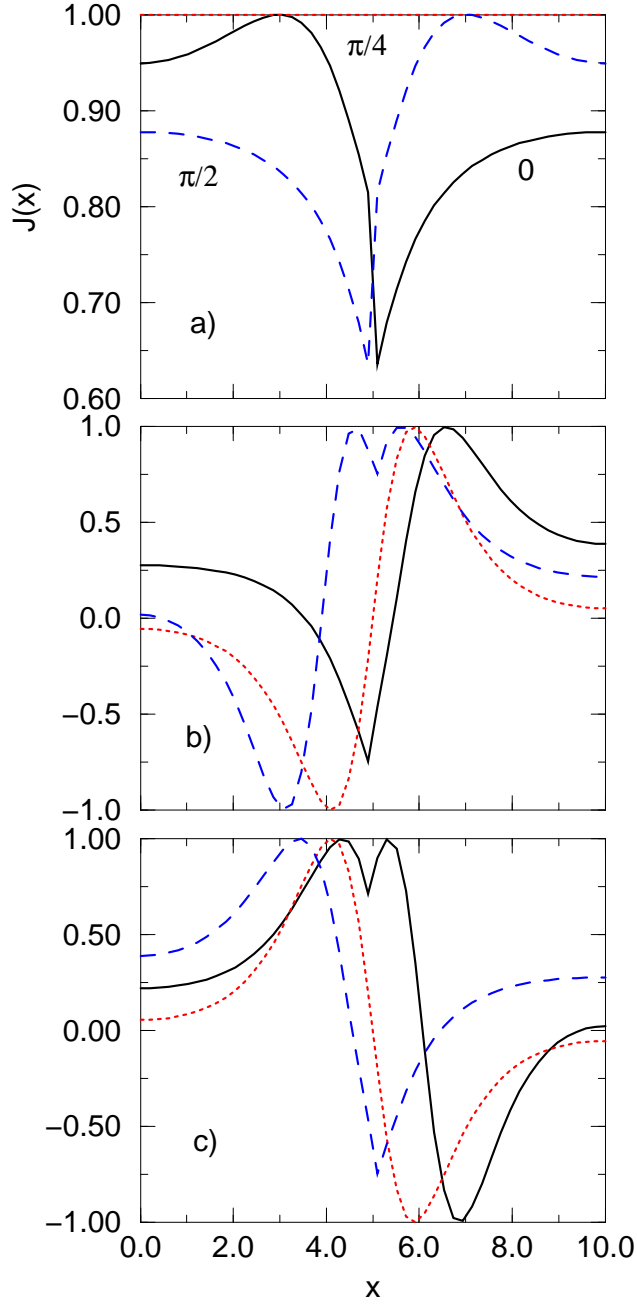


FIG. 4. The current density distribution $J(x)$ of the vortex solutions (a) $n = 0$, (b) $n = -1$, and (c) $n = 1$, at $\alpha = 0, \pi/4, \pi/2$; for a corner junction of isotropic p -wave and s -wave superconductors, with length $L = 10$, and maximum overlap external current I^{ov} .

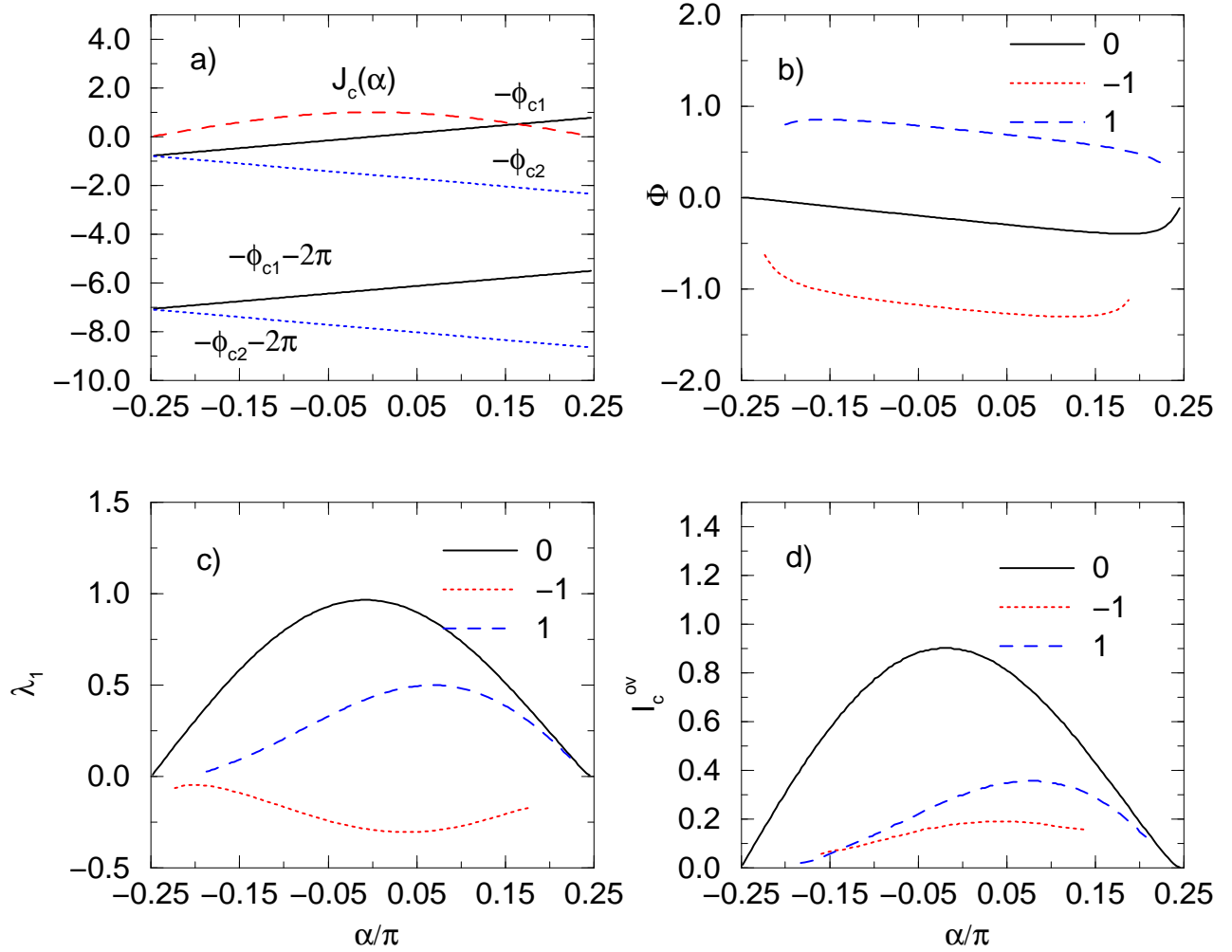


FIG. 5. The same as in Fig. 2. The pairing symmetry of the triplet superconductor is $B_{1g} \times E_u$.

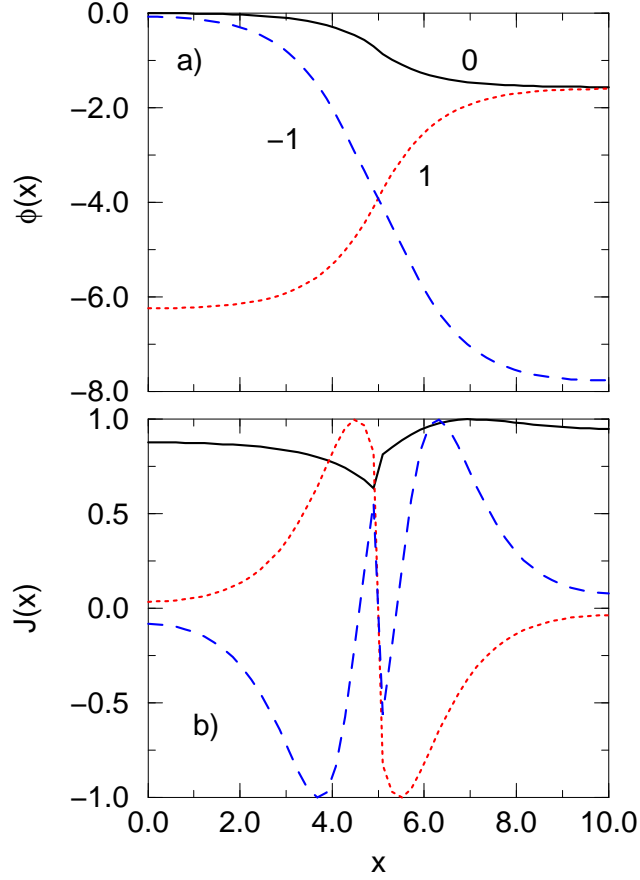


FIG. 6. (a) The phase distribution of the vortex solutions at $\alpha = 0$, for a junction with length $L = 10$, and zero external current $I^{ov} = 0$. (b) The corresponding current density at the maximum external current. The pairing symmetry of the triplet superconductor is $B_{1g} \times E_u$.

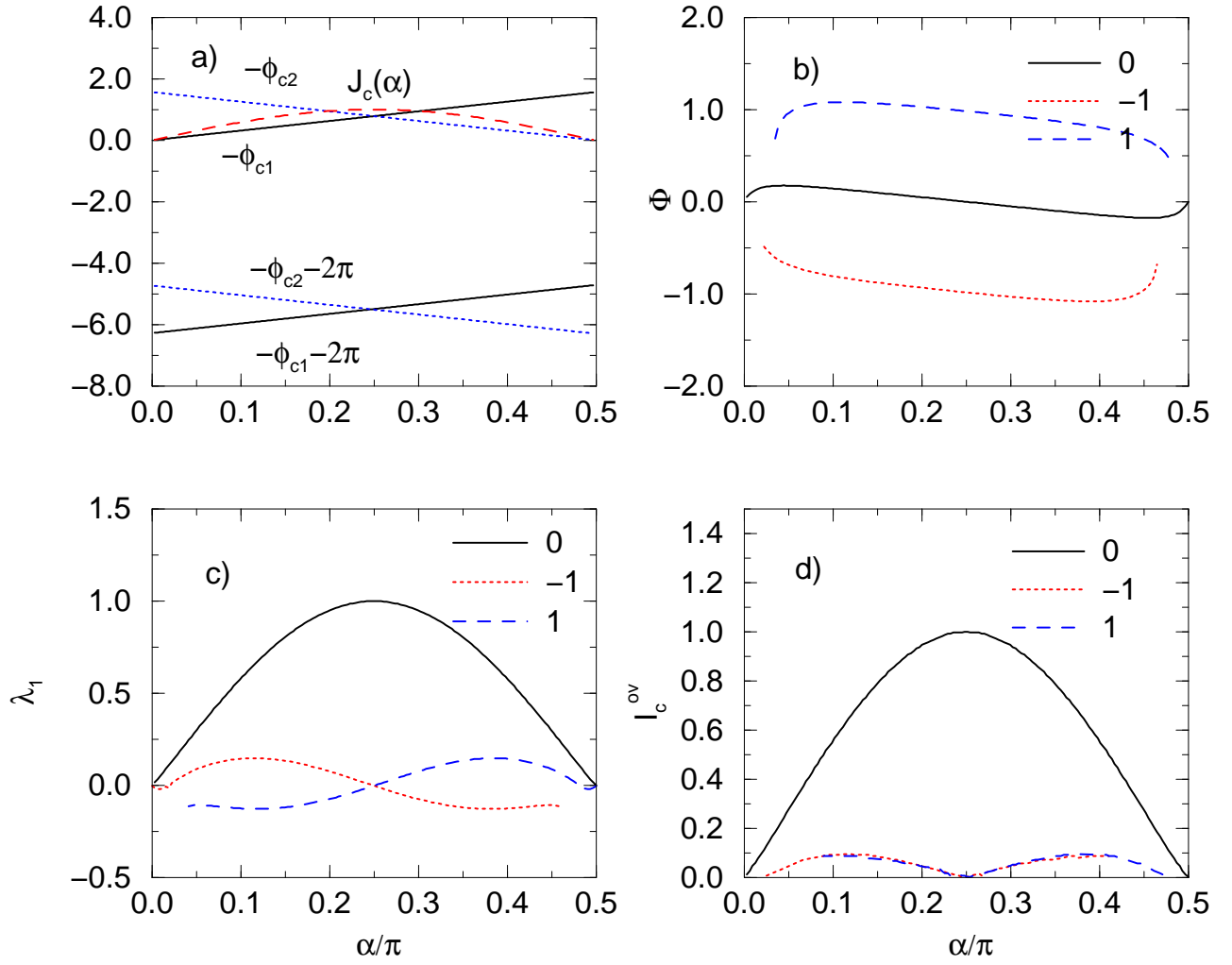


FIG. 7. The same as in Fig. 2. The pairing symmetry of the triplet superconductor is $B_{2g} \times E_u$.

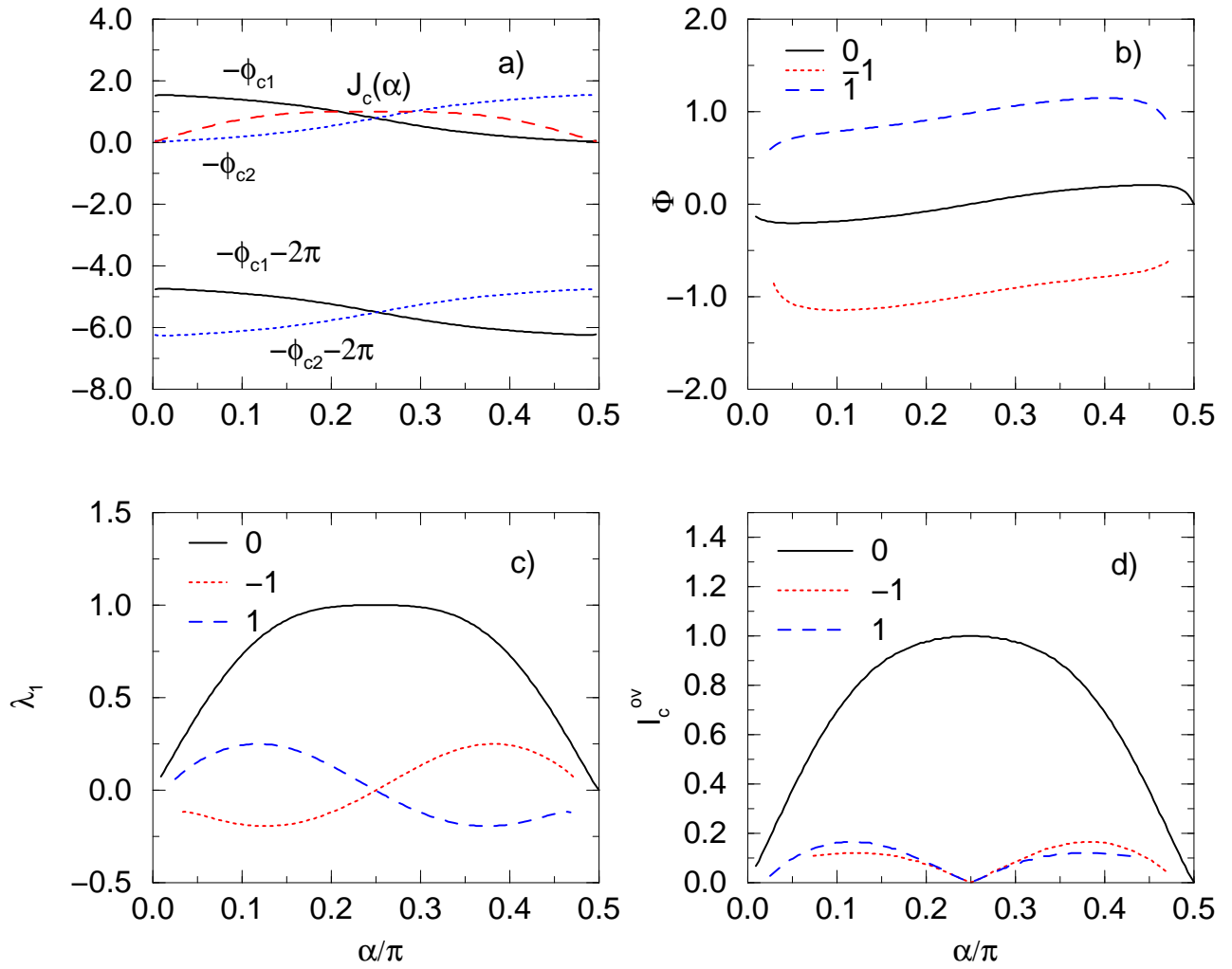


FIG. 8. The same as in Fig. 2. The pairing symmetry of the triplet superconductor is nodal p wave.

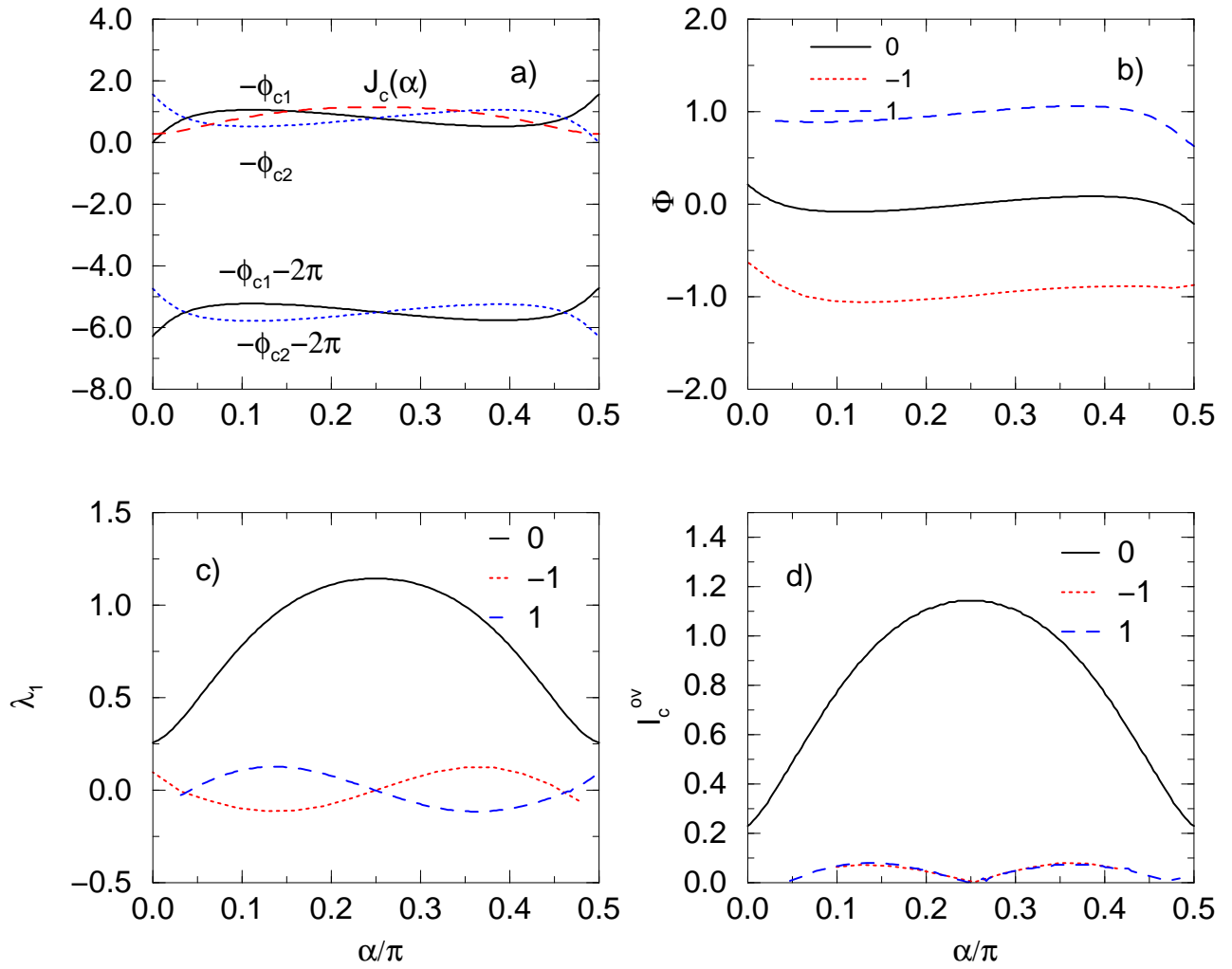


FIG. 9. The same as in Fig. 2. The pairing symmetry of the triplet superconductor is nodeless p wave.

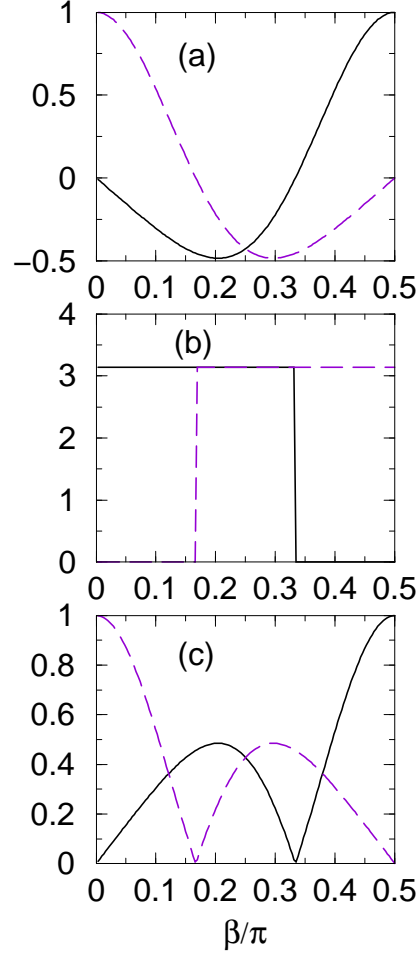


FIG. 10. (a) The effective two-dimensional order parameter $\mathbf{d} = \hat{\mathbf{z}} \sin \beta \cos(\pi \cos \beta)$ versus the polar angle β for adjacent junction edges as solid and dashed lines. (b) The characteristic phase ϕ_{c1} (ϕ_{c2}) as a solid (dashed line). (c) The Josephson critical current densities \tilde{J}_{c1} , \tilde{J}_{c2} for adjacent junction edges as solid and dashed lines.

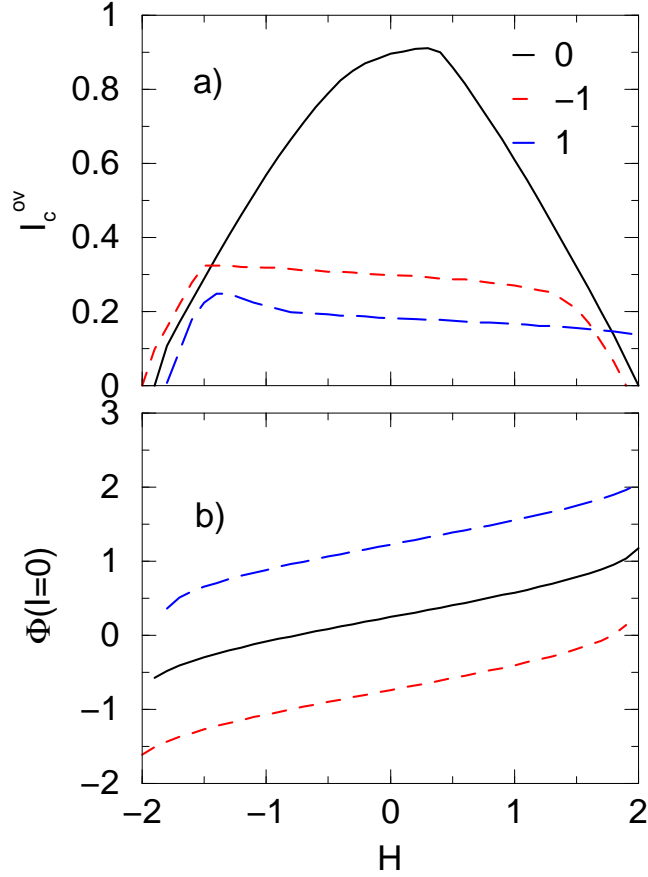


FIG. 11. (a) The variation of the overlap I_c^{ov} critical current with the magnetic field H for the three vortex solutions $n = 0, 1, -1$. (b) The spontaneous magnetic flux Φ as a function of the magnetic field H , for the $0, -1, 1$ mode solutions, for a junction of length $L = 10$, and the angle $\alpha = 0$. The pairing symmetry of the triplet superconductor is isotropic p wave.

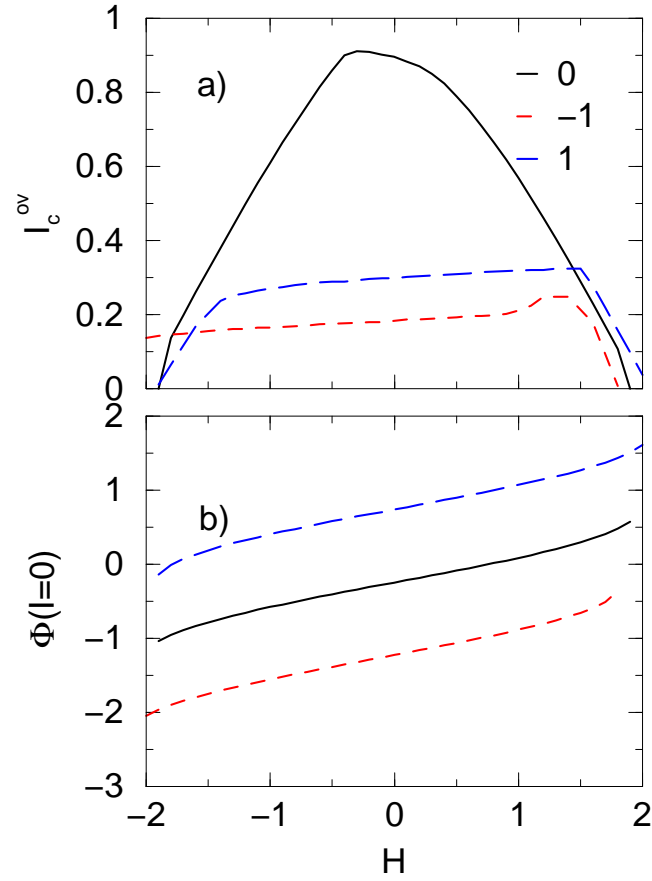


FIG. 12. The same as in Fig. 10. The pairing symmetry of the triplet superconductor is $B_{1g} \times E_u$.